American Mineralogist, Volume 62, pages 747–755, 1977

Mullite: a substituted alumina

WARRINGTON E. CAMERON

Department of Mineralogy and Petrology
University of Cambridge, Cambridge, England

Abstract

Mullite solid-solution can be represented by the formula $Al_{4+2x}Si_{2-2x}O_{10-x}$, $Z = 1$, where x is the number of oxygen atoms missing per unit cell. The presence of a miscibility gap between sillimanite ($x < 0.04$) and siliceous mullite ($x = 0.17$) suggests that their different ordering schemes, deduced from SAED studies, may be the underlying cause, and that the true end-member is aluminum-rich. Supporting evidence lies in the lengthening of the modulation wavelength, interpreted as a systematic coarsening of mullite antiphase domains, with increasing Al content. The concomitant trend toward greater sharpness and complexity of the superstructure reflections defining domain size may be a consequence simply of chemical fluctuations near domain boundaries, but is also very likely to result from the long-range ordering of oxygen vacancies. Mullite cell dimensions vary almost linearly with composition, and when extrapolated beyond those for the most aluminous one found in this study (76 mole percent Al_2O_3; $x = 0.59$), fall very close to those of a metastable polymorph of alumina, ι–Al_2O_3. A structure for this mullite end-member is postulated, and a hypothetical phase diagram given for the system Al_2SiO_5–Al_2O_3 in the absence of corundum.

Introduction

Wyckoff *et al.* (1926) observed that the X-ray powder patterns of sillimanite and mullite are remarkably similar. Subsequent investigations (*e.g.* Agrell and Smith, 1960) showed that it is possible to distinguish the two minerals by such a technique, but only by careful measurement of the lattice parameters. As expected, single-crystal X-ray work produced very similar structures: both are made up of AlO_6 chains parallel to the c axis and cross-linked by $(Si,Al)O_4$ tetrahedra. Sillimanite has Si and Al ordered on the tetrahedral sites (Burnham, 1962), giving rise to a doubled c repeat (2×2.9 A). Mullite solid-solution, generally acknowledged to lie between the compositions $3Al_2O_3 \cdot 2SiO_2$ and $2Al_2O_3 \cdot SiO_2$, is arrived at by the substitution scheme $2\,Si^{4+} + O^{2-} \rightleftarrows 2Al^{3+} + \square$. In structure determinations of the 2.9 A cell, ordering on the sillimanite-type $(Al,Si)^{iv}$ sites could not be detected, but it was found that a new tetrahedral site containing aluminum is adopted adjacent to the position where each oxygen atom is lost (Sadanaga *et al.*, 1962; Burnham, 1964a). Burnham (1964b) pointed out that, given such a scheme, there was no structural reason why mullite solid-solution should not extend fully between sillimanite and alumina. In practice, the Al-rich limit is determined by the encroachment of the corundum stability field (Welch, 1961) or the liquidus (Aramaki and Roy, 1962) at about 1850°C, but silica-rich compositions ought all to occur in nature, in pyroxene–hornfels or sanidinite facies rocks.

The fact that the most siliceous naturally occurring mullite found so far (57 mole percent Al_2O_3) coexists, apparently stably, with a sillimanite of composition 51 mole percent Al_2O_3 (Cameron, 1976a, specimen 109671) poses a major problem. One might have expected that a small amount of solid solution, say to 55 mole percent Al_2O_3, would be energetically more favored than the relatively large number of oxygen vacancies required to give mullites near 3:2 in composition at a similar temperature. Natural mullites, however, have a very restricted field of solid solution (from 57–60 mole percent Al_2O_3), and in one example, specimen Al 37y, a mullite of composition 59 mole percent Al_2O_3 has exsolved sillimanite, leaving a more aluminous mullite host (Cameron, 1976b). These observations suggest that the short-range ordering schemes of sillimanite and mullite are fundamentally different in type, and the end member on which the mullite structure is based has to be sought

elsewhere. This paper aims to show that mullite can be described in terms of a Si-substituted polymorph of alumina.

Experimental

Mullites were purified in 20 percent HF followed by 1:1 HCl solution and then separated from contaminant phases, if necessary, by Clerici solution. Densities were obtained by the sink-float method in the same liquid. Chemical analyses were done by electron microprobe following the method of Sweatman and Long (1969), except for specimens 6, 8, and 10 (below), which were too fine-grained and were analyzed by X-ray fluorescence by the method described by Norrish and Hutton (1969). Standard deviations in alumina contents are considered to be ± 0.5 mole percent. Cell parameters were refined using a program similar to that of Burnham (1965) from powder data obtained by scanning at 0.125°/min between 56–77° 2θ, Cu$K\alpha$ radiation, with Si metal as standard. Transmission electron microscopy was carried out at 100 kV with an A.E.I. EM-6G instrument on ground samples evaporated from alcohol onto Cu grids. An EMMA-4 analysis was kindly carried out on the synthetic alumina by G. Cliff using the method described by Lorimer and Cliff (1976). Specimen descriptions follow; those with partial chemical analyses are from Cameron (1977), in which complete analyses and cell dimensions may be found.

Synthetic mullites

1. Fused mullite (No. 3) melted in argon, then quenched (70.7 mole percent Al_2O_3).
2. Commercial fused mullite (69.7 mole percent Al_2O_3, including 1.0 weight percent TiO_2).
3. Commercial fused mullite, rapidly cooled zone (69.2 mole percent Al_2O_3).
4. As No 3 but more slowly cooled (67.8 mole percent Al_2O_3).
5. As No. 3, single crystal from center of ingot (66.7 mole percent Al_2O_3).
6. Commercial sintered mullite, heated at 1720–1750°C for 12+ hr. (65.6 mole percent Al_2O_3).
7. Mullite from Corhart refractory (63.8 mole percent Al_2O_3, including 1.1 weight percent TiO_2).
8. Sintered mullite made by heating 3:2 mix of γ-Al_2O_3 and SiO_2 gel at 1750°C for 8 hr (63.8 mole percent Al_2O_3).
9. Mullite crystallized from $10CaO{:}30Al_2O_3{:}60SiO_2$ melt at 1550°C (62.9 mole percent Al_2O_3).
10. Mullite separated from commercial aluminosilicate refractory obtained by heating kaolinite with small amounts of fluxes at 1530°C for 25 hr (60.4 mole percent Al_2O_3, including 1.4 weight percent Fe_2O_3).

FM Forster Mullite (Agrell and Smith, 1960; 68.3 mole percent Al_2O_3).

58480 Type specimen of D-mullite of Agrell and Smith. From Corhart refractory (66 mole percent Al_2O_3 including 2–3 weight percent TiO_2).

92552t Quenched top of specimen No. 2 (71.4 mole percent Al_2O_3, including 1.3 weight percent TiO_2).

Q1 Mullite No. 2 with sufficient Al_2O_3 added to make a bulk composition of 75 mole percent Al_2O_3. Melted in argon then quenched.

Q2 Mullite No. 3 with sufficient Al_2O_3 added to make a bulk composition of 76 mole percent Al_2O_3. Melted in argon then quenched.

Rα, Rβ α– and β–mullites of Rooksby and Partridge (1939). Assumed to be 3:2 and 2:1 respectively but from cell-dimension data, 62.5 and 65.0 mole percent Al_2O_3.

Naturally occurring mullites

92423 From corundum–mullite–spinel buchite, 2½ ft. from the contact, Sithean Sluaigh, Argyllshire (Smith, 1965). Analysis gives Al_2O_3 68.3 weight percent, SiO_2 28.3 weight percent, TiO_2 0.7 weight percent, Fe_2O_3 2.6 weight percent, Cr_2O_3 0.08 weight percent. Equivalent to 60.0 mole percent Al_2O_3.

S18001a From mullite buchites, Isle of Mull.

76398 Complete analyses given in Cameron (1976c).

109671 Mullite from sillimanite–mullite–cordierite buchite, Mull (Cameron, 1976a).

Al 37y Mullite with exsolved sillimanite, Bushveld Complex (Cameron, 1976b).

Sillimanite

100622 Most Al-rich sillimanite interpreted as crystallizing from liquid. From Asama Volcano, Japan (51.4 mole percent Al_2O_3

with 2.6 weight percent Fe_2O_3, Cameron 1976c).

Five and six figure numbers refer to specimens in the Harker Collection, Cambridge. S18001a was provided by the Institute of Geological Sciences, London.

Solid solution

From results of a study of natural and synthetic mullites (Cameron, 1977), it was found that those which crystallized from liquids can have compositions ranging from 57 to 71 mole percent Al_2O_3, depending on the temperature of crystallization and cooling rate. For a given cooling rate the alumina content increases with temperature, but rapid quenching at the high-alumina end (*e.g.* of specimen 3) produces even more aluminous mullites (specimen 1). Mullites formed by reaction in the solid state have temperature-dependent compositions over a more restricted range, 60–66 mole percent Al_2O_3, the higher value being that at which melting commences. It was noted that there was no clustering of mullite compositions around the 3:2 or 2:1 stoichiometries, in spite of a widespread belief to the contrary begun by Bowen and Greig (1924). They did not acid-treat and analyze the 3:2 mix fired at temperatures just below the liquidus, but simply assumed that, because it appeared homogeneous optically, the composition of the mullite formed must have been identical to that of the starting material. In fact, it would have been about 66 mole percent Al_2O_3.

The mullite solid-solution scheme as deduced from the structure determinations requires the number of cations to be fixed at six for the c = 2.9 A cell. An appropriate formula would be

$$Al_2^{vi}\,[Al_{2+2x}Si_{2-2x}]^{iv}\,O_{10-x}$$

with Z = 1 and x the number of possible O_c atoms (Burnham, 1964a) missing per unit cell. To check that the formula is valid over the known composition range, a number of careful density measurements were made; the data are shown in Figure 1. The Fe-, Ti-bearing mullites[1] are slightly denser than pure binary mullites for a given value of x, but the results are in remarkable agreement with the theoretical density curve calculated for Al + Si = 6, using cell-

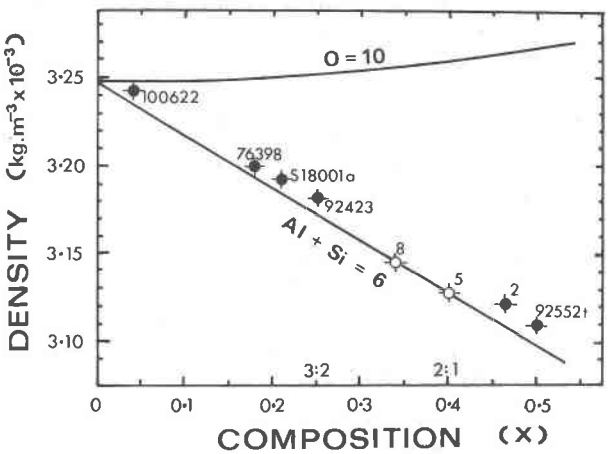

Fig 1. Experimentally determined (●,○) and calculated values (——) for mullite density based on a fixed number of cations per unit cell with oxygen vacancies (Al+Si = 6) or a fixed number of O atoms with interstitial cations (O = 10).

● = Fe,Ti-bearing sillimanite and mullites

○ = Fe_2O_3 + TiO_2 < 0.5 wt %

dimension data from specimens 3–5, 9, and the Brandywine Springs sillimanite (Cameron, 1976*a*, 1977).

The silica-rich limit of the solid-solution series (x = 0.17) occurs where mullite coexists with sillimanite. The alumina-rich end was investigated by attempting to crystallize mullite from above the liquidus at bulk compositions between 75 and 100 mole percent Al_2O_3. Precipitated alumina was added to specimens 2 and 3, and the finely-ground mixture was held at temperatures above 2100°C in argon on a Mo strip furnace for 1–2 minutes and then quenched rapidly (at about 1000°C/sec.). Only two runs produced any mullite: one with a bulk composition of 75 mole percent Al_2O_3 yielded quench mullite (Q1) and a glass of similar composition, and a second with 76 mole percent Al_2O_3 and about 1 mole percent TiO_2 impurity gave mullite Q2 (30%), corundum (60%) and glass (10%). Microprobe analyses of these and more conventional mullites with limiting compositions are given in Table 1.

Cell dimensions for mullites in the composition range 60–71 mole percent Al_2O_3 vary linearly with composition (Fig. 2), but are subject to small systematic increases when Fe and/or Ti is in solid solution. Chemical composition and not Al–Si order is evidently the main variable (*c.f.* Aramaki and Roy, 1962). Continuing lines of best fit beyond the Q1 and Q2 *a* and *b* cell parameters shows that they probably cross near x = 0.63, 79 mole percent Al_2O_3; more Al-

[1] Fe and Ti were considered to be substituting for Al^{vi}, on size and charge criteria and the fact that pleochroism in mullite is probably due to charge transfer between Fe^{2+} and Ti^{4+}, which can only take place along the MO_6 chains.

Table 1. Limiting compositions and cell dimensions for mullite solid solution

	Natural mullite 109671	Quenched mullite 1	Quenched Al-doped mullites Q1	Q2	ι-Al_2O_3
Al_2O_3	68.3	80.4	82.9	84.3	-
SiO_2	30.5	19.6	16.3	15.7	∿1.0
TiO_2	0.7	n.d.	0.8	n.d.	n.d.
Fe_2O_3	0.5	n.d.	n.d.	n.d.	n.d.
Total	100.0	100.0	100.0	100.0	
Mole % Al_2O_3 + TiO_2 + Fe_2O_3	57.3(5)*	70.7(5)	75.2(5)	76.0(5)	99.0(5)
x	0.17(1)	0.49(1)	0.57(1)	0.59(1)	0.98(1)
Cell Dimensions					
a(Å)	7.5251(4)	7.6040(4)	7.6367(4)	7.634(1)	7.688(2)
b(Å)	7.5873(5)	7.6763(5)	7.6656(4)	7.660(1)	7.688(2)
c(Å)	2.8862(2)	2.8900(2)	2.8980(2)	2.8960(4)	2.901(1)

Microprobe analyses are the average of 10 points, corrected to 100%.
n.d. = below the detection limit.
* *Parenthesized figures represent the estimated standard deviation (esd) in terms of least units cited for the value to their immediate left, thus 57.3(5) indicates an esd of 0.5.*

rich mullites could either be tetragonal or orthorhombic.

Reports of silica-free compounds with mullite-type structures provided the vital clue for the solution of the mullite problem offered here. Foster (1959) synthesized a tetragonal polymorph of alumina which had an X-ray powder pattern very similar to that of mullite. The phase, known now as ι-Al_2O_3, is probably identical to that prepared by Perrotta and Young (1974). Saalfeld (1962) and Du Vigneaud (1974) described a similar phase but with orthorhombic symmetry, however, in the latter case, the published diffractometer trace shows none of the expected peak splittings. After a number of attempts, the phase free from impurities could be prepared only in a fashion generally similar to that described by Foster. EMMA-4 analyses (Table 1) of bundles of single crystals showed that the Si content was 1.0 ± 0.5 weight percent and Na below the detection limit, found to be about 2 percent. Varying amounts of silica were added to the cryolite–alumina mixtures, but the products all contained other Al_2O_3 polymorphs in much greater abundance.

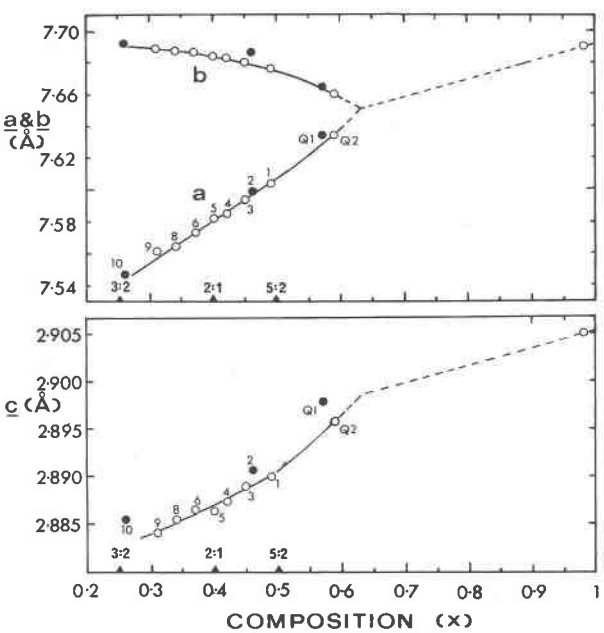

Fig. 2. Variation of lattice parameters with mullite composition, with speculative extrapolations to the pure alumina end-member. Symbols as in Fig. 1.

Although the ι-Al_2O_3 crystals were only 0.1 × 1 μm, tolerably accurate cell dimensions could be determined from broadened X-ray peaks (Table 1). The values are similar to those obtained by refinement of Perrotta and Young's data and considerably less than those of Du Vigneaud, whose sample may have contained significant amounts of sodium. There was no evidence for splitting of the 120 and 210 peaks, nor at higher angles, for 250-520 and 251-521, intense reflections split by about 1° 2θ in the case of aluminous mullites. On powder X-ray evidence alone, it would appear that ι-Al_2O_3, as prepared, is tetragonal; following this tenuous assumption, an interpolation of the cell dimension–composition relationship is made in Figure 2. If a and b simply cross, one can predict that the orthorhombic form of ι-Al_2O_3 should have a∼7.74A, b∼7.60A, in very reasonable agreement with Saalfeld's data. Regardless of the symmetry of the end-member phase, the cell parameter–composition relation expressed in Figure 2 accords with the idea of complete solid-solution between ι-Al_2O_3 and siliceous mullite.

Direct evidence for a orthorhombic ⇄ tetragonal transformation at 79 mole percent Al_2O_3 (at liquidus temperatures) is, of course, lacking, and is unlikely ever to be demonstrated, as ι-Al_2O_3 decomposes readily to other polymorphs of alumina. Tetragonal mullites, assumed to have compositions in the 3:2–2:1 range, have, however, been described (Ossaka, 1961). Their preparation from highly reactive gels heated at relatively low temperatures suggests that they are metastable intermediates which yield normal mullite at elevated temperatures and after sufficiently long heating times.

Ordering scheme

In each small (2.9A) mullite cell, there are four cations in tetrahedral coordination. One has, there-

fore, the possibility of fully-ordered phases at, for example, $x = 0.25$ (3:2), $x = 0.75$ (11:2), and particularly $x = 0.50$ (5:2), but no evidence was found for them. Superlattice reflections would be expected to appear at simple fractions of h, k, and l, as in sillimanite. Two sets of reflections at irrational positions in reciprocal space characterize mullite (Scholz, 1955; Agrell and Smith, 1960), but have been ignored so far in structure determinations. They are typical of modulated structures and are most likely to originate from the ordering of oxygen vacancies, and as a consequence, Al and Si to some extent. The more intense set consists of pairs of reflections which are diffuse in some specimens and sharp in others, parallel to a^* about absent sillimanite superlattice positions. This was first interpreted as being characteristic of an antiphase domain structure with domain boundaries parallel to (100) and a shift vector $\mathbf{c}/2$ by Smith and McConnell (1966), and has since received support from a study by high-resolution electron microscopy (Nakajima *et al.*, 1975).

A systematic survey revealed that the superstructure reflections are sensitive to chemical composition, essentially a function of temperature of crystallization, and to a lesser extent, thermal history. Figure 3 summarizes the styles of extra reflections, best seen in $\{h0l\}$ sections, in going from the silica-rich limit of mullite solid-solution to pure alumina (a → h). Figures 3a and b are from naturally occurring specimens and show the development of a reasonably well correlated domain structure involving the large ($c = 5.8$A) cell from $x = 0.17$ (57.5 mole percent Al_2O_3) to the Al-rich limit ($x = 0.20$, 60 mole percent Al_2O_3). The extra reflections of synthetic mullites with compositions lying between specimens 92423 and 58480 (Fig. 3c) are similar, varying only in the length of the **s** vector, as defined by Bown and Gay (1958). Specimen 58480 is the type D-mullite of Agrell and Smith (1960) and has superstructure reflections identical in intensity, diffuseness, and spacing to those of specimen Rβ_{ec} used for Burnham's structure determination. Figure 3d is from Forster Mullite, Agrell and Smith's type specimen of S-mullite. Going to more aluminous compositions (Fig. 3e), a second set of spots appears, paired about the average (2.9A cell) reflections and analogous to the 'f' reflections in calcic plagioclase. Weak, second-order 'e'-type reflections are seen, as well as streaks approximately parallel to c^*. An identical pattern was obtained from specimen 92552t of similar composition.

Specimen Q1 (Fig. 3f) is one stage more complex and appears to represent the interaction of a second antiphase domain structure parallel to c^*. This may be a manifestation of the enigmatic second set of extra reflections which, in the composition range characteristic of commercially produced mullites, are paired with $l = \pm 0.16$ about non-integral k values. In the quench specimen, however, the reflections are positioned at $l \pm 0.085$ about the former 'f's, corresponding to an almost doubled repeat. Figure 3g (specimen Q2) shows a truly magnificent array of very sharp superstructure reflections: the second-order spots are now split into four, the 'f' reflections three, and second-order 'f' reflections, five. Streaks joining the 'e'- and 'f'-type reflections have been replaced by a number of discrete maxima and a new set of streaks parallel to c^*.

No fundamental explanation is offered for the precise changes in position and intensity of the extra reflections in $\{h0l\}$ sections described above. It is clear, though, that there are two aspects of ordering in mullite. The increasing intensity and sharpness of the reflections at $l = 1/2$ imply greater degrees both of short-range correlations between atoms and/or vacancies in the upper and lower halves of the 5.8A cell, as well as long-range modulations (giving rise to what is interpreted as an antiphase domain structure) with a period of $1/2\mathbf{s}$, on a register totally independent of the conventional unit cell. Secondly, the appearance of the extra intensity at integral values of l means that there must be chemical variations on the scale of a single domain in the most aluminum-rich mullites. Fluctuations in composition might be anticipated near domain boundaries. Although the SAED patterns suggest a very well defined mullite "supercell" with dimensions $a = 1/2\mathbf{s}$ and $c = 5.8$A, it should be remembered that over 10^6 of them are being sampled, and one is dealing with a statistical problem. The likelihood of ever being able to describe the actual structure (as distinct from the average structure) on an atomic scale is remote: the domain structure is more subtle than simple blocks of 1½ or 2 7.6 × 7.7 × 5.8A cells arranged along the c direction in proportions determined by bulk composition.

The variation of the **s** vector with composition is particularly informative, however (Fig. 4). To a reasonable approximation, a straight line is obtained for mullites with similar thermal histories (those with $0.30 < x < 0.47$). Ones with $x > 0.47$ are rapidly quenched and therefore may be expected to deviate slightly from the line of best fit, assuming of course that there is some rationale for an $\mathbf{s}$–x relationship. At the silica-rich end, the three specimens have very

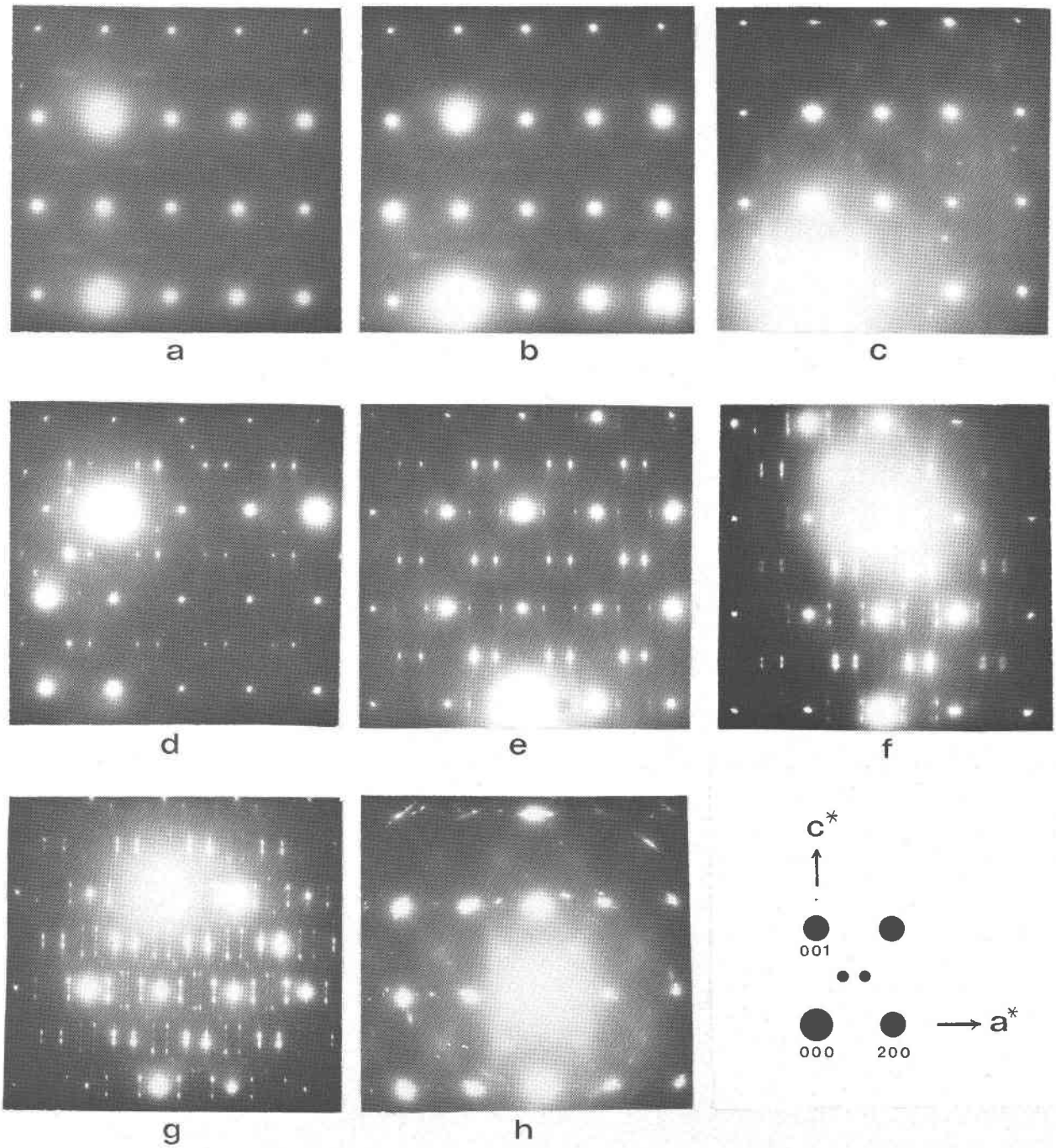

Fig. 3. {*h*0*l*} reciprocal-lattice sections of mullites, showing the variation in type of the superlattice reflections with increasing alumina content. (a) specimen 76398, (b) specimen 92423, (c) specimen 58480, (d) Forster Mullite, (e) specimen 1, (f) specimen Q1, (g) specimen Q2, (h) ι-Al_2O_3.

different thermal histories: sample 10 cooled in a matter of hours while the Sithean Sluaigh specimen would probably have taken years. The Bushveld specimen with exsolved sillimanite, Al 37y, has possibly the slowest terrestrial cooling rate so far encountered.

The domain repeat across the solid-solution series varies from only 9.5 to 14A, but it is significant that the width of the domains, for a consistent thermal history (typical of commercial synthetic mullites), increases with aluminum content. This suggests that the

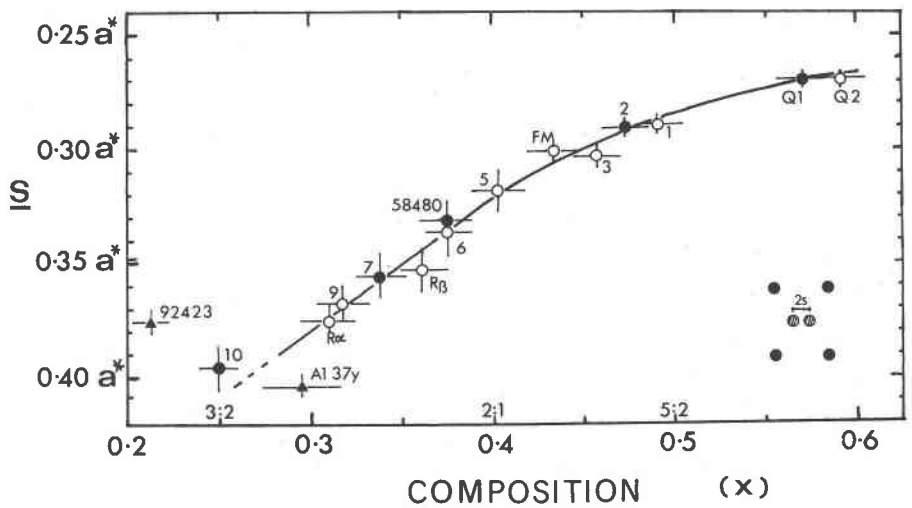

Fig. 4. Variation in s vector, as measured in {*h*0*l*} reciprocal lattice sections, with mullite composition. Symbols as in Fig. 1, including ▲ = naturally occurring mullites.

structural end member is being approached. It is an interesting fact that if the straight portion of the line in Figure 4 is extrapolated to $x = 1$, the s vector becomes very nearly zero, defining a structure with the mullite ordering scheme at the pure alumina composition. There is, as yet, no theoretical justification for such an interpretation, but it is very appealing in its simplicity.

Structure of ι-Al_2O_3 and mullite

The indifferent {*h*0*l*} diffraction patterns obtained from ι-Al_2O_3 (Fig. 3h) show very diffuse reflections centered on *h* odd, *l* odd (for the 5.8A cell), similar in position to those of sillimanite. Given the structure of mullite as determined from the average reflections, one can speculate on the Al^{iv} and O_c positions in ι-Al_2O_3. Both species lie at $z = ½$ in the small cell, and there are two of the special Al* (Burnham, 1964a) positions and two shared vacant O_c sites per unit cell. Such a compound cannot help but flagrantly disregard the aluminum avoidance principle (Loewenstein, 1954) and so might be expected to decompose to α-Al_2O_3 at lower temperatures (1200°C according to Foster, 1959). Arranging the oxygen vacancies in what seems the most energetically favorable way results in the section shown in Figure 5a. A doubled *c* repeat is very likely if the opposite array alternates (Fig. 5b), giving a possible structure for a fully-ordered orthorhombic form. The diffraction pattern shows very diffuse intensity at $l = ½$, suggesting that the tetragonal phase is close to the inversion temperature. Besides the oxygen vacancies, there is another possibility for ordering: the Al* positions could equally well have been chosen in the opposite orientations. The ι-Al_2O_3 phase synthesized in this work probably has both kinds of disorder, which gives an average 2.9A cell of tetragonal symmetry.

Non-random substitution of Si + ½O for Al* in the ordered form of ι-Al_2O_3 would explain to some

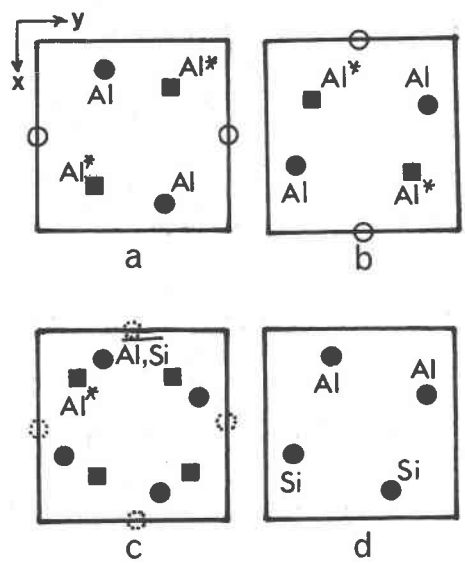

Fig. 5. Distribution of Al^{iv} and Si^{iv} at height $z = ½$ in the small (c = 2.9A) cell. ● = sillimanite-type site, ■ = new aluminium position (Al*) adjacent to vacant oxygen site (○) found in mullite. (a) predicted for ι-Al_2O_3, (b) ι-Al_2O_3, other half of 5.8A cell, (c) average mullite structure, (d) sillimanite.

extent the position and sharpness of the extra reflections in mullite (Fig. 5c). Aluminous mullites near $x = 0.5$ have about one Al* per 2.9A cell. Minimization of local charge imbalance is most easily achieved by arranging these atoms diagonally, as in ι-Al_2O_3, in the 5.8A cell. This structure, continued in the x direction only into the next unit cell would constitute one of the antiphase alternatives. A shift of origin by **c**/2 at the domain boundary gives the other. This model is over-simplified (it ignores the alternative Al* distribution mentioned above), but it does allow for a high degree of short-range order. The ordering scheme is obviously entirely different from that of sillimanite (Fig. 5d). As more Si is substituted, there are fewer oxygen vacancies so a correlation between them becomes more difficult, and as a result, the superstructure reflections become more diffuse and domain widths smaller. The composition of mullite is, however, strongly temperature-dependent, and the apparent increase in disorder with lowering temperature of crystallization could be due partly to the extremely slow diffusion rate of aluminum. The apparently highly-ordered domain structure in specimen Q2 would have been quenched in at 2000°C, whereas D-mullite 58480 probably cooled slowly from 1800°C.

Phase diagram

The closest approach to equilibrium compositions for mullite solid-solution at different temperatures might be expected where crystallization has taken place from a slowly cooling liquid. The parageneses of specimen 9 and naturally occurring mullites give information on the position of the solidus, although it must be recognized that mullite coexisted with a multicomponent, silica-rich liquid at the time. An attempted summary of the findings of this paper is portrayed on the pseudobinary phase diagram for the system Al_2SiO_5–Al_2O_3 (Fig. 6). A possible orthorhombic ⇄ tetragonal inversion is shown, but the geometry of the phase boundaries toward the pure alumina composition can only be speculative, as they are cut by the stable field of corundum + liquid (dashed in the figure) at high temperatures and corundum + mullite in the sub-solidus region. Quenching from bulk compositions more siliceous than 2:1 at temperatures near that of the peritectic results in mullite (3), while much more rapid quenching from well above the liquidus produces mullite metastably until about 76 mole percent Al_2O_3 is reached. One explanation, in view of the flatness of the corundum liquidus, is that mullite has a melting maximum near 75 mole percent Al_2O_3. There is ample evidence from the powder and

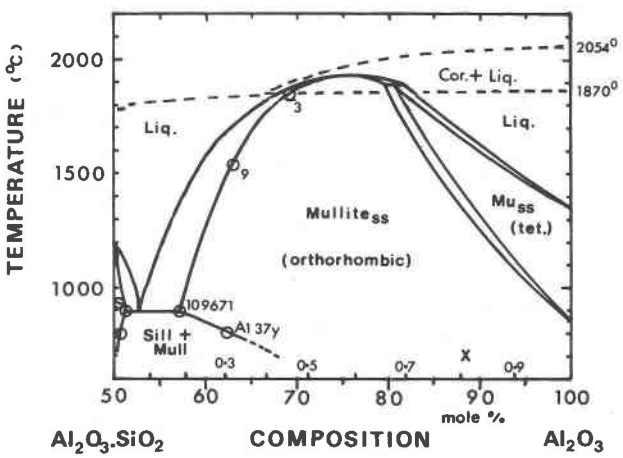

Fig. 6. Possible phase diagram for the system Al_2SiO_5–Al_2O_3 in the presence of a multicomponent liquid with the field of mullite + corundum removed. Phase relations at compositions on the Al-rich side of 80 mole % Al_2O_3 are hypothetical.

single-crystal diffraction results that there are no ordered compounds of simple stoichiometry in the system.

Acknowledgments

Dr. J. D. C. McConnell invited my attention to the existence of ι-Al_2O_3 and many other problems concerned with the system Al_2O_3–SiO_2. I am also most grateful for his and Professor C. W. Burnham's comments on the manuscript. Dr. S. O. Agrell kindly provided some of the specimens.

References

Agrell, S. O. and J. V. Smith (1960) Cell dimensions, solid solution, polymorphism, and identification of mullite and sillimanite. *J. Am. Ceram. Soc., 43,* 69–76.

Aramaki, S. and R. Roy (1962) Revised phase diagram for the system Al_2O_3–SiO_2. *J. Am. Ceram. Soc., 45,* 229–242.

Bowen, N. L. and J. W. Greig (1924) The system Al_2O_3–SiO_2. *J. Am. Ceram. Soc., 7,* 238–254.

Bown, M. G. and P. Gay (1958) The reciprocal lattice geometry of the plagioclase feldspar structures. *Z. Kristallogr., 111,* 1–14.

Burnham, C. W. (1962) The crystal structure of sillimanite. *Carnegie Inst. Wash. Year Book, 61,* 135–139.

——— (1964a) Crystal structure of mullite. *Carnegie Inst. Wash. Year Book, 63,* 223–227.

——— (1964b) Compositional limits of mullite, and the sillimanite-mullite solid solution problem. *Carnegie Inst. Wash. Year Book, 63,* 227–229.

———(1965) Refinement of lattice parameters using systematic correction terms. *Carnegie Inst. Wash. Year Book, 64,* 200–202.

Cameron, W. E. (1976a) Coexisting sillimanite and mullite. *Geol. Mag., 113,* 497–514.

——— (1976b) Exsolution in 'stoichiometric' mullite. *Nature, 264,* 736–738.

———(1976c) A mineral phase intermediate in composition between sillimanite and mullite. *Am. Mineral., 61,* 1025–1026.

——— (1977) Composition and cell dimensions of mullite. *Am. Ceram. Soc. Bull.,* in press.

Du Vigneaud, P. H. (1974) Existence of mullite without silica. *J. Am. Ceram. Soc., 57,* 224.

Foster, P. A. (1959) The nature of alumina in quenched cryolite–alumina melts. *J. Electrochem. Soc., 106.* 971–975.

Loewenstein, W. (1954) The distribution of aluminum in the tetrahedra of silicates and aluminates. *Am. Mineral., 39,* 92–96.

Lorimer, G. W. and G. Cliff (1976) Analytical electron microscopy of minerals. In H.-R. Wenk, Ed., *Electron Microscopy in Mineralogy,* p. 506–519. Springer-Verlag, Berlin.

Nakajima, Y., N. Morimoto and E. Watanabe (1975) Direct observation of oxygen vacancy in mullite, 1.86 $Al_2O_3 \cdot SiO_2$ by high resolution electron microscopy. *Proc. Japan. Acad. 51,* 173–178.

Norrish, K. and J. T. Hutton (1969) An accurate X-ray spectrographic method for analysis of a wide range of geological samples. *Geochim. Cosmochim. Acta, 33,* 431–453.

Ossaka, J. (1961) Tetragonal mullite-like phase from co-precipitated gels. *Nature, 191,* 1000–1001.

Perrotta, A. J. and J. E. Young, Jr. (1974) Silica-free phases with mullite type structures. *J. Am. Ceram. Soc., 57,* 405–407.

Rooksby, H. P. and J. H. Partridge (1939) X-ray study of natural and artificial mullites. *J. Soc. Glass Technol., 23,* 338–346.

Saalfeld, H. (1962) A modification of Al_2O_3 with sillimanite structure. In *Transactions VIIIth Int. Ceram. Congr.,* p. 71–74. The Organizing Committee of the VIIIth Int. Ceram. Congr., Copenhagen.

Sadanaga, R., M. Tokonami and Y. Takéuchi (1962) The structure of mullite, $2Al_2O_3 \cdot SiO_2$, and relationship with the structures of sillimanite and andalusite. *Acta Crystallogr. 15,* 65–68.

Scholze, H. (1955) Zum Sillimanit–Mullit–Problem. *Ber. deut. keram. Ges., 32,* 381–385.

Smith, D. G. W. (1965) The chemistry and mineralogy of some emery-like rocks from Sithean Sluaigh, Strachur, Argyllshire. *Am. Mineral., 50,* 1982–2022.

Sweatman, T. R. and J. V. P. Long (1969) Quantitative electron-probe microanalysis of rock-forming minerals. *J. Petrol., 10,* 332–379.

Welch, J. H. (1961) Observations on composition and melting behavior of mullite. In *Transactions VIIth Int. Ceram. Congr.* p. 197–206. British Ceramic Society, London.

Wyckoff, R. W. G., J. W. Greig and N. L. Bowen (1926) The X-ray diffraction patterns of mullite and of sillimanite. *Am. J. Sci., 11,* 459–472.

Manuscript received, August 5, 1976; accepted for publication, January 17, 1977.